Acta Mechanica Solida Sinica, Vol. 25, No. 5, October, 2012 ISSN 0894-9166
Published by AMSS Press, Wuhan, China

RATE DEPENDENT STRESS-STRETCH RELATION OF DIELECTRIC ELASTOMERS SUBJECTED TO PURE SHEAR LIKE LOADING AND ELECTRIC FIELD**

Shaoxing Qu[1,2*] **Ke Li**[1,2] **Tiefeng Li**[1,2] **Hanqing Jiang**[3] **Miao Wang**[4] **Zhenhua Li**[1]

([1] *Department of Engineering Mechanics, Zhejiang University, Hangzhou* 310027*, China*)
([2] *Soft Matter Research Center (SMRC), Zhejiang University, Hangzhou* 310027*, China*)
([3] *School for Engineering of Matter, Transport and Energy, Arizona State University, Tempe, AZ* 85287*, USA*)
([4] *Department of Physics, Zhejiang University, Hangzhou* 310027*, China*)

Revision received 29 April 2012

ABSTRACT The performance of dielectric elastomer (DE) transducers is significantly affected by viscoelastic relaxation-induced electromechanical dissipations. This paper presents an experimental study to obtain the rate dependent stress-stretch relation of DE membranes (VHB^{TM}9473) subjected to pure shear like loading and electric loading simultaneously. Stretching rate dependent behavior is observed. The results also show that the tensile force decreases as the voltage increases. The observations are compared with predictions by a viscoelastic model of DE. This experiment may be used for further studies of dynamic electromechanical coupling properties of DEs.

KEY WORDS dielectric elastomer, viscoelastic, electromechanical coupling, membranes

I. INTRODUCTION

As a specific class of materials in the electroactive polymers (EAP) family, dielectric elastomers (DEs) were first introduced into the electromechanical transducers technology in 1990s[1–5]. Since the discovery of an efficient way to obtain voltage-induced large deformation with strain beyond 100% by Pelrine et al. in 2000[6], DEs have been studied extensively by numerous groups[7–15] due to their excellent overall performance, such as light weight, high efficiency, large voltage induced deformation, high energy density, etc. DE transducers can convert mechanical energy to or from electrical energy. The basic structure of a DE transducer is shown in Fig.1. The DE membrane is sandwiched between two compliant electrodes (carbon grease). Subjected to a voltage, electrons will flow from one electrode to the other through external circuit. The attraction between charges with different signs on the electrodes will contract the DE membrane in thickness and stretch it in area. This electromechanical coupling effect has inspired various designs and analysis of soft DE transducers as actuators, generators

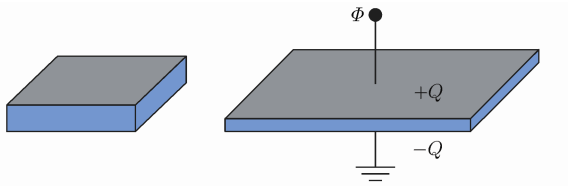

Fig. 1 Schematic diagram of a DE transducer, i.e., DE membrane sandwiched between two soft electrodes.

* Corresponding author. E-mail: squ@zju.edu.cn

** Project supported by the National Natural Science Foundation of China (No. 10832009), the Program for New Century Excellent Talents in University (NCET-08-0480), Zhejiang Provincial Natural Science Foundation of China (No. Z1110057), and the Fundamental Research Funds for the Central Universities.

and sensors.

Equilibrium thermodynamics of DE coupling the large deformation and electric field have been studied recently[16–19]. Suo made a comprehensive review about the current progress with the theory of DE[20]. Most of the previous studies on DE focus on elastic behavior with the effect of viscoelasticity neglected. Recently, studies show that the dissipation mechanisms such as viscoelasticity and current leakage highly affect the performances of DE transducers[21–23]. Based on nonequilibrium thermodynamics theory, Zhao et al. developed an approach to construct models of DEs undergoing dissipative processes, including viscoelastic, dielectric and conductive relaxation[24].

DE transducers usually work under dynamic mechanical and electrical loadings. In this work, the rate-dependent electromechanical coupling properties of DE subjected to mechanical and electric loadings simultaneously are investigated experimentally, and a newly developed viscoelastic model[24] is adopted to explain the experimental results. The current study is very helpful to analyze and understand the performance of DE transducers. The work is presented as following. The pure shear loading is verified in §II. In §III, experiments are carried out to obtain the voltage effect on the stretching rate dependent stress-stretch curves of the DE membrane. In §IV, a viscoelastic constitutive model is described. Experimental results and those predicted by the viscoelastic model are compared in §V.

II. PURE SHEAR LIKE LOADING

Pure shear test, i.e., constrained test or planar test, is a widely-used method to characterize the mechanical properties of soft materials[25]. Figure 2 shows a schematic diagram of pure shear testing. The specimen is a thin rectangular sheet with a uniformly distributed tensile loading in 1- direction along its upper and lower sides. The horizontal displacement along its lateral sides is restrained. The deformation along the thickness direction (3-direction) is free. Theoretically, deformation in the whole specimen is homogeneous. In practice, it is suggested that the length of the long side is at least 8 times greater than that of the short side in order to achieve globally homogeneous deformation. The incompressive materials subjected to the above pure shear loading possess the deformation gradient $\boldsymbol{F}$ as

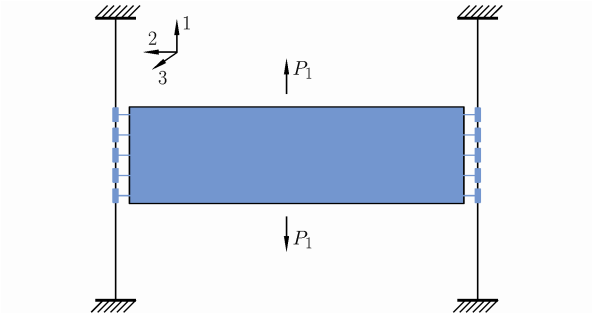

Fig. 2 Schematic diagram of pure shear testing.

$$\boldsymbol{F} = \begin{bmatrix} \lambda & 0 & 0 \\ 0 & 1 & 0 \\ 0 & 0 & \dfrac{1}{\lambda} \end{bmatrix} \tag{1}$$

where λ is the stretch along the tensile loading direction. The velocity gradient tensor L can be written as

$$\boldsymbol{L} = \dot{\boldsymbol{F}}\boldsymbol{F}^{-1} = \boldsymbol{D} + \boldsymbol{W} = \frac{\dot{\lambda}}{\lambda}\begin{bmatrix} 1 & 0 & 0 \\ 0 & 0 & 0 \\ 0 & 0 & -1 \end{bmatrix} \tag{2}$$

where $\dot{\boldsymbol{F}}$ represents the deformation gradient rate, $\boldsymbol{D}$ the symmetric part of $\boldsymbol{L}$, $\boldsymbol{W}$ the anti-symmetric part of $\boldsymbol{L}$, and $\dot{\lambda}$ the stretching rate. Clearly, the maximum shear deformation rate is equal to the principal deformation rate. Moreover, the normal deformation rate associated with the plane of the maximum shear deformation rate is zero.

In our experiments, the specimens are first prestretched in the horizontal direction and then the tensile forces along the upper and lower sides, as well as the electric field, are applied. This can be used to model an approximate pure shear condition. Numerical analysis has shown that the result of the resultant force-displacement relation with prestretch of 2.5 is very similar to that of the pure shear loading.

III. EXPERIMENT

Specimens are made of a commercially available acrylic elastomer (VHB$^{\text{TM}}$9473) membrane, sandwiched between two soft electrodes (carbon conductive grease, MG$^{\text{TM}}$mechanicals, 846-80G). As described in §II, the pure shear like loading is applied on the specimens. The testing processes are schematically shown in Fig.3. Figure 3(a) represents the reference state of DE. The initial dimensions of the dielectric membrane are $L_1 = 7.9$ mm, $L_2 = 40$ mm, and $L_3 = 0.25$ mm. First, the specimens are stretched in 2-(horizontal) direction until the stretch ratio, λ_{2p}, reaches 2.5. In order to keep the width nearly unchanged in the experiments, the upper and lower sides are clamped tightly by plastic boards, as shown in Fig.3(b). Then tensile forces are applied on the upper and lower sides using the testing machine (ZWICK$^{\text{TM}}$z2.5), as well as a voltage on the opposite electrodes (Fig.3(c)).

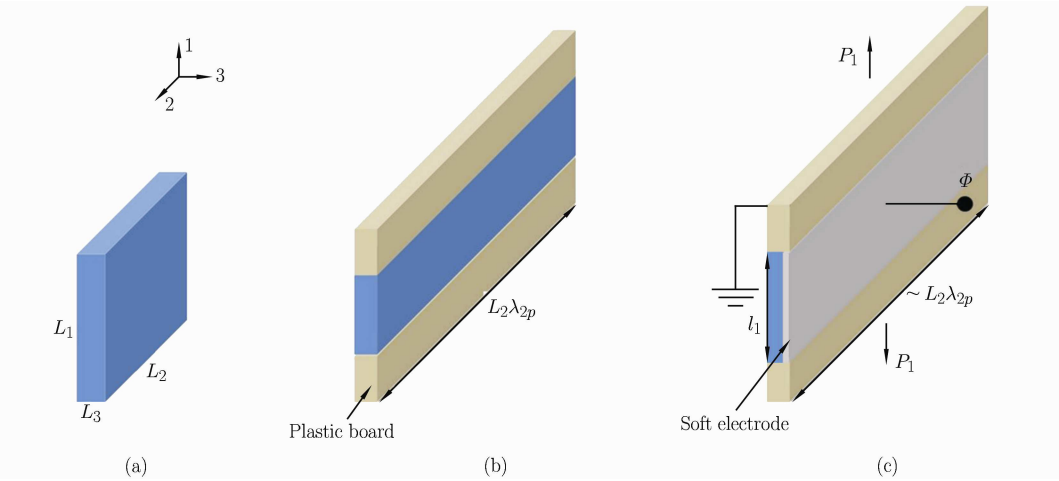

Fig. 3. Pure shear like testing process of DE in three states. (a) Reference state. The membrane is of length L_1 in 1-direction, L_2 in 2-direction, and L_3 in 3-direction (the thickness direction); (b) Prestretched state. The membrane is prestretched in 2-direction and is clamped by rigid frames. Electrodes are coated on both sides of membrane; (c) Actuated state. In response to the voltage Φ and forces P_1 applied, DE membrane expands in 1-direction and contracts in 3-direction. The width (2-direction) is assumed to keep unchanged.

In our displacement controlled experiment, three stretching rates are adopted, i.e., 50 mm/min, 200 mm/min, and 800 mm/min. For each stretching ratewe adjust the voltage to 0 V, 800 V, 1200 V, and 1600 V. The high voltage amplifier (TREK$^{\text{TM}}$610E) is connected to the electrodes with the conducting wires. When the specimen is attached to the testing machine, it is stretched to a certain value of l_{10} in 1-direction and then the high voltage amplifier is turned on (to make sure that no compression force occurs in the specimen). Before loading, the maximum displacement $d_{1\max}$ is set up with the testing machine, and the voltage applied on DE through the thickness direction can be adjusted with high voltage amplifier. During deformation, the DE membrane expands in 1-direction and contracts in thickness direction. However, the width (2-direction) keeps almost constant. When the displacement reaches $d_{1\max}$, the test will end up automatically. The curves of tensile forces (P_1) vs. displacements (d_1) can be recorded. In our experiment, totally 12 curves of force-displacement are obtained. For convenience, we use nominal stress s_1 ($s_1 = P_1/L_2L_3$), and stretch ratio λ_1 [$\lambda_1 = (l_{10} + d_1)/L_1$] instead of tensile force and displacement. The curves of $s_1 = s_1(\lambda_1)$ obtained from experiment are plotted in the right part of Fig.6 in §V.

IV. A VISCOELASTIC MODEL

Response of DE subjected to mechanical or electric loading is time dependent, which leads to the development of the dissipative constitutive model for DE based on nonlinear equilibrium thermodynamics[20,24]. In this general model, when DE is subjected to mechanical loads P_1, P_2, P_3 along 1-, 2-, 3-directions,

and a voltage Φ through 3-direction, the free energy density function is written as

$$W = W\left(\lambda_1,\, \lambda_2,\, \lambda_3,\, \tilde{D},\, \xi_1,\, \xi_2,\, \cdots\right) \tag{3}$$

where $\lambda_1 = l_1/L_1$, $\lambda_2 = l_2/L_2$, and $\lambda_3 = l_3/L_3$ are defined as the stretches of DE along 1-, 2-, and 3-directions, respectively. $\tilde{D} = Q/L_1L_2$ is defined as the nominal electric displacement. $(\xi_1,\, \xi_2,\, \cdots)$ represent the internal variables that describe the degrees of freedom associated with dissipative processes of DE. The state of dielectric is characterized by λ_1, λ_2, λ_3, $\tilde{D}$, and $(\xi_1,\, \xi_2,\, \cdots)$. It is known that the external mechanical loadings and electric loading will do work through λ_1, λ_2, λ_3, and $\tilde{D}$, which are therefore called kinematic variables. Assuming that the system is in mechanical and electrostatic equilibrium, thermodynamic theory can give the following equations of state of DE:

$$s_1 = \frac{\partial W\left(\lambda_1,\, \lambda_2,\, \lambda_3,\, \tilde{D},\, \xi_1,\, \xi_2,\, \cdots\right)}{\partial \lambda_1} \tag{4}$$

$$s_2 = \frac{\partial W\left(\lambda_1,\, \lambda_2,\, \lambda_3,\, \tilde{D},\, \xi_1,\, \xi_2,\, \cdots\right)}{\partial \lambda_2} \tag{5}$$

$$s_3 = \frac{\partial W\left(\lambda_1,\, \lambda_2,\, \lambda_3,\, \tilde{D},\, \xi_1,\, \xi_2,\, \cdots\right)}{\partial \lambda_3} \tag{6}$$

$$\tilde{E} = \frac{\partial W\left(\lambda_1,\, \lambda_2,\, \lambda_3,\, \tilde{D},\, \xi_1,\, \xi_2,\, \cdots\right)}{\partial \tilde{D}} \tag{7}$$

and the thermodynamic inequality

$$\sum_i \frac{\partial W\left(\lambda_1,\, \lambda_2,\, \lambda_3,\, \tilde{D},\, \xi_1,\, \xi_2,\, \cdots\right)}{\partial \xi_i}\delta\xi_i \le 0 \tag{8}$$

where $s_1 = P_1/L_2L_3$, $s_2 = P_2/L_1L_3$, $s_3 = P_3/L_1L_2$ are defined as the nominal normal stresses, $\tilde{E} = \Phi/L_3$ is defined as the nominal electric field.

If DE is subjected to pure shear loading as demonstrated by Fig.2, and a voltage through the thickness direction, the equations of state of DE and thermodynamic inequality are obtained following the same process as described above. The thermodynamic theory requires that

$$\delta F \le P_1\delta l_1 + \Phi\delta Q \tag{9}$$

Divide both sides of Eq.(9) by the volume of DE, $L_1L_2L_3$, the thermodynamic inequality becomes

$$\delta W \le s_1\delta\lambda_1 + \tilde{E}\delta\tilde{D} \tag{10}$$

Consider the incompressibility of DE, $\lambda_1\lambda_2\lambda_3 = 1$, and λ_2 as constant, we adopt the free energy density function W as

$$W = W\left(\lambda_1, \lambda_2 = \text{const}, \tilde{D}, \xi_1, \xi_2, \cdots\right) \tag{11}$$

Substituting Eq.(11) into Eq.(10), the thermodynamics inequality can be rewritten as

$$\left(\frac{\partial W}{\partial \lambda_1} - s_1\right)\delta\lambda_1 + \left(\frac{\partial W}{\partial \tilde{D}} - \tilde{E}\right)\delta\tilde{D} + \sum_i \frac{\partial W}{\partial \xi_i}\delta\xi_i \le 0 \tag{12}$$

We assume that DE is in mechanical and electrostatic equilibrium. The equations of state of DE and thermodynamic inequality can be obtained from Eq.(12) as

$$s_1 = \frac{\partial W\left(\lambda_1,\, \lambda_2 = \text{const},\, \tilde{D},\, \xi_1,\, \xi_2,\, \cdots\right)}{\partial \lambda_1} \tag{13}$$

$$\tilde{E} = \frac{\partial W\left(\lambda_1,\, \lambda_2 = \text{const},\, \tilde{D},\, \xi_1,\, \xi_2,\, \cdots\right)}{\partial \tilde{D}} \tag{14}$$

$$\sum_i \frac{\partial W\left(\lambda_1,\, \lambda_2 = \text{const},\, \tilde{D},\, \xi_1,\, \xi_2,\, \cdots\right)}{\partial \xi_i}\delta\xi_i \le 0 \tag{15}$$

In our work, only the dissipative process of viscoelastic relation is considered. We adopted the same rheological model as Zhao et al.'s[24] to illuminate the viscoelastic behavior of the elastomer. As shown in Fig.4, the elastomer is modeled as two networks of polymers, represented by the spring at the top, and the spring and the dashpot at the bottom. The same mechanical forces are applied on the two networks. The shear modulus of the top spring is defined as μ_R, and the shear modulus of the bottom spring as $\mu_U - \mu_R$. The relaxation time τ is related to the viscosity of the dashpot η and the stiffness of the bottom spring as

$$\tau = \frac{\eta}{\mu_U - \mu_R} \tag{16}$$

The net deformation of the networks subjected to pure shear loading and electric field are represented by in-plane stretches (λ_1, $\lambda_2 = \text{const}$). For the network represented by the top spring, λ_1 is the stretch associated with the deformation of the spring while λ_2 keeps unchanged. For that represented by the spring and the dashpot at the bottom, the net stretches due to the deformation of the spring and the dashpot are described as

$$\lambda_1 = \lambda_1^e \xi_1, \ \lambda_2 = \lambda_2^e \xi_2 = \text{const} \tag{17}$$

where (λ_1^e, λ_2^e) are the stretches associated with the bottom spring, and (ξ_1, ξ_2) are the stretches associated with the dashpot.

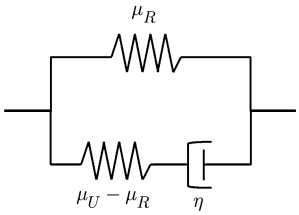

Fig. 4. A viscoelastic model consisting of springs and dashpot for DE. μ_U is the shear modulus of the top spring. $\mu_U - \mu_R$ is the shear modulus of the bottom, and η is the viscosity of the dashpot.

The free-energy density function of the DE, W, is still defined as the sum of the elastic energy and the electrical energy. The elasticity of the networks is represented by the Gent free-energy density function. Consequently, the free-energy density function takes the form:

$$\begin{aligned} W = & -\frac{\mu_R J_{\lim}}{2} \ln\left(1 - \frac{\lambda_1^2 + \lambda_2^2 + \lambda_1^{-2}\lambda_2^{-2} - 3}{J_{\lim}}\right) \\ & -\frac{(\mu_U - \mu_R) J_{\lim}}{2} \ln\left(1 - \frac{\lambda_1^2\xi_1^{-2} + \lambda_2^2\xi_2^{-2} + \lambda_1^{-2}\lambda_2^{-2}\xi_1^2\xi_2^2 - 3}{J_{\lim}}\right) + \frac{\tilde{D}^2}{2\varepsilon}\lambda_1^{-2}\lambda_2^{-2} \end{aligned} \tag{18}$$

where $J_{\lim}$ is a materials constant associated with elastic deformation. The first term in the right side of Eq.(18) is the elastic energy of the network represented by the top spring, the second term is the elastic energy of the network represented by the bottom spring, and the third term represents the electrical energy. Here it is assumed that the electrical energy possesses the same form as a dielectric liquid, with a constant permittivity ε. μ_R, μ_U, $J_{\lim}$ and τ (or η) can be obtained by fitting the experimental data.

Substituting Eq.(18) into Eqs.(13) and (14), we obtain:

$$\begin{aligned} s_1 = & \frac{J_{\lim}\mu_R(\lambda_1 - \lambda_1^{-3}\lambda_2^{-2})}{J_{\lim} + 3 - \lambda_1^2 - \lambda_2^2 - \lambda_1^{-2}\lambda_2^{-2}} \\ & + \frac{J_{\lim}(\mu_U - \mu_R)(\lambda_1\xi_1^{-2} - \lambda_1^{-3}\lambda_2^{-2}\xi_1^2\xi_2^2)}{J_{\lim} + 3 - \lambda_1^2\xi_1^{-2} - \lambda_2^2\xi_2^{-2} - \lambda_1^{-2}\lambda_2^{-2}\xi_1^2\xi_2^2} - \frac{\lambda_1^{-3}\lambda_2^{-2}\tilde{D}^2}{\varepsilon} \end{aligned} \tag{19}$$

$$\tilde{E} = \frac{\lambda_1^{-2}\lambda_2^{-2}\tilde{D}}{\varepsilon} \tag{20}$$

The above equations (19) and (20) constitute the equations of state of the model represented by the free-energy density function (18). In order to satisfy the thermodynamic inequality (15), we choose the kinetic model as $\mathrm{d}\xi_1/\mathrm{d}t = -\eta^{-1}\partial W/\partial\xi_1$, and $\mathrm{d}\xi_2/\mathrm{d}t = -\eta^{-1}\partial W/\partial\xi_2$ following Zhao et al.'s work[24]. Substituting Eq.(18) into the above evolution equations, we obtain the kinetic model as follows:

$$\frac{\mathrm{d}\xi_1}{\mathrm{d}t} = \frac{J_{\lim}}{\tau}\left(\frac{\lambda_1^2\xi_1^{-3} - \lambda_1^{-2}\lambda_2^{-2}\xi_1\xi_2^2}{J_{\lim} + 3 - \lambda_1^2\xi_1^{-2} - \lambda_2^2\xi_2^{-2} - \lambda_1^{-2}\lambda_2^{-2}\xi_1^2\xi_2^2}\right) \tag{21}$$

$$\frac{\mathrm{d}\xi_2}{\mathrm{d}t} = \frac{J_{\lim}}{\tau}\left(\frac{\lambda_2^2\xi_2^{-3} - \lambda_1^{-2}\lambda_2^{-2}\xi_2\xi_1^2}{J_{\lim} + 3 - \lambda_1^2\xi_1^{-2} - \lambda_2^2\xi_2^{-2} - \lambda_1^{-2}\lambda_2^{-2}\xi_1^2\xi_2^2}\right) \tag{22}$$

V. RESULTS COMPARISON

We fit the viscoelastic model described in §IV to pure shear like tests conducted on acrylic elastomer (VHB^{TM}9473) at several loading rates, i.e., 50 mm/min, 200 mm/min, and 800 mm/min. The following set of parameters are obtained: $\mu_U = 88.5$ kPa, $\mu_R = 19.2$ kPa, $\tau = 20$ s, and $J_{\lim} = 180$. Figure 5 shows a good agreement between the experimental data and the curves predicted by the viscoelastic model with the above parameters.

The same values of the set of parameters, μ_R, μ_U, $J_{\lim}$ and τ, are also used to compare the experimental data and those obtained by the viscoelastic model subjected to four different voltages, i.e., 0 V, 800 V, 1200 V, and 1600 V. The value of the permittivity ε is taken as $3\varepsilon_0$, where ε_0 is the vacuum permittivity.

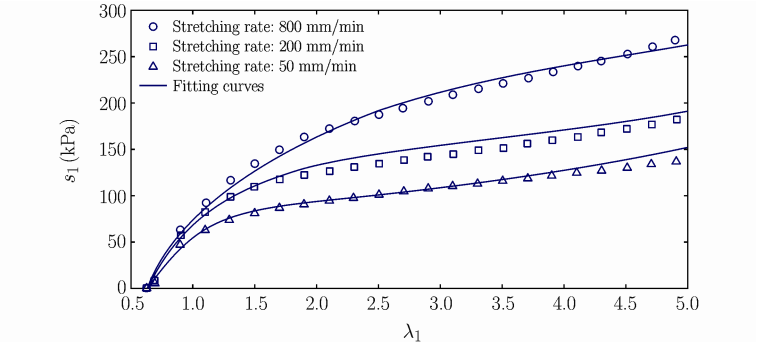

Fig. 5. The viscoelastic model is fitted to experimental data of pure shear like tension of a DE under three stretching rates.

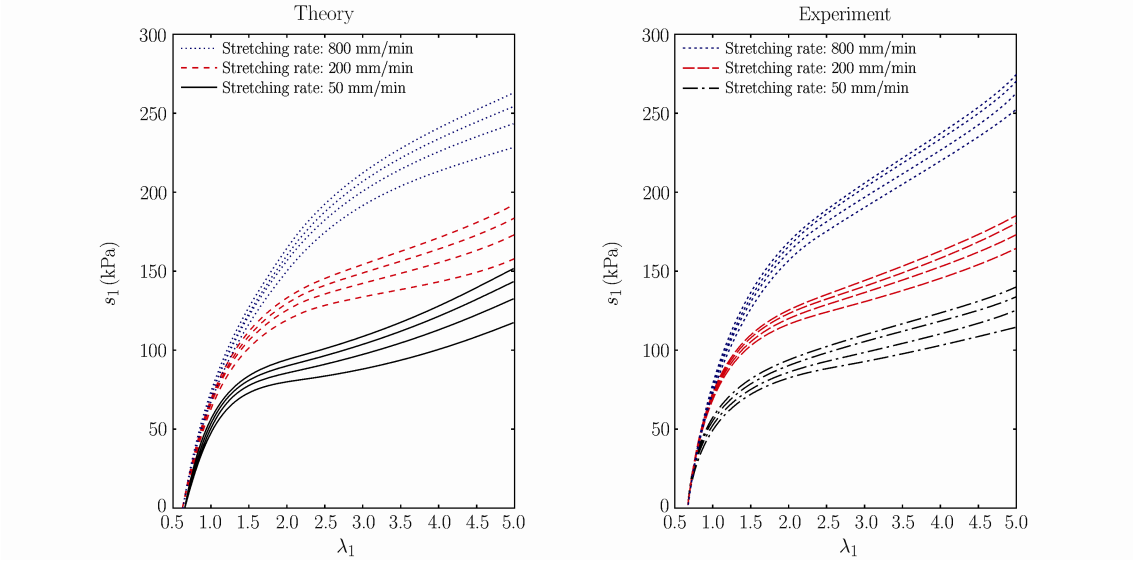

Fig. 6. Stress-stretch curves obtained by experiment (right) and predicted by the viscoelastic model (left).

For acrylic elastomer (VHB^{TM}), permittivity ε usually falls in 3-4ε_0 using standard testing method. The experimental data are plotted in the right part of Fig.6, while those predicted by the viscoelastic model in the left part. In Fig.6, different color represents different stretching rate. For each set with the same stretching rate, there are four curves indicating the applied voltage from 0 V to the highest value of 1600 V. Figure 6 shows clearly that the results by the viscoelastic model agree well with the experimental observations, as well as the same effect trends for both stretching rate and electric field. As the stretch increases, apparent difference of the stress induced by electric field occurs between experiment and theory. It is expected that as the stretch increases, the permittivity ε does not keep constant again. Stretching rate and electric field dependent viscosity of DE should be investigated in the future.

VI. RESULTS COMPARISON

Experimental studies on the dynamic electromechanical response of a DE membrane subjected to pure shear like loadings and electric field are performed. The DE membrane expands in plane along the loading direction when subjected to a voltage through the thickness direction, which leads to the decreasement of the tensile force with the voltage. The stress-stretch curves display strong stretching rate and electric field dependence. The electric field dependence is well explained by Maxwell stress effect due to the voltage applied. The stretching rate dependence indicates clearly the dissipation process attributing to viscoelastic relaxation. A rheological model consisting of springs and dashpot are adopted within the nonequilibrium thermodynamic theory, which yields the equations of state of DE. Experimental data and results predicted by the viscoelastic model agree reasonably well. Results comparison between experiment and theory brings forward the future study on stretching rate and electric field dependent viscosity of DE.

References

[1] Hirai,T., Nemoto,H., Hirai,M. and Hayashi,S., Electrostriction of highly swollen polymer gel: Possible application for gel actuator. *Journal of Applied Polymer Science*, 1994, 53(1): 79-84.

[2] Heydt,R., Kornbluh,R., Pelrine,R. and Mason,V., Design and performance of an electrostrictive-polymer-film acoustic actuator. *Journal of Sound and Vibration*, 1998, 215(2): 297-311.

[3] Pelrine,R.E., Kornbluh,R.D. and Joseph,J.P., Electrostriction of polymer dielectrics with compliant electrodes as a means of actuation. *Sensors and Actuators A: Physical*, 1998, 64(1): 77-85.

[4] Zanna,J.J., Nguyen,H.T., Parneix,J.P., Ruffié,G. and Mauzac,M., Dielectric properties of side chain liquid crystalline elastomers: influence of crosslinking on side chain dynamics. *The European Physical Journal B—Condensed Matter and Complex Systems*, 1999, 10(2): 345-351.

[5] Liang,C., Sun,F.P. and Rogers,C.A., Coupled electro-mechanical analysis of adaptive material systems — determination of the actuator power consumption and system energy transfer. *Journal of Intelligent Material Systems and Structures*, 1994, 5(1): 12-20.

[6] Pelrine,R., Kornbluh,R., Pei,Q. and Joseph,J., High-speed electrically actuated elastomers with strain greater than 100%. *Science*, 2000, 287(5454): 836-839.

[7] Pelrine,R., Kornbluh,R., Joseph,J., Heydt,R., Pei,Q. and Chiba,S., High-field deformation of elastomeric dielectrics for actuators. *Materials Science and Engineering: C*, 2000, 11(2): 89-100.

[8] Pelrine,R., Kornbluh,R. and Kofod,G., High-strain actuator materials based on dielectric elastomers. *Advanced Materials*, 2000, 12(16): 1223-1225.

[9] Wissler,M. and Mazza,E., Electromechanical coupling in dielectric elastomer actuators. *Sensors and Actuators a-Physical*, 2007, 138: 384-393.

[10] Moscardo,M., Zhao,X., Suo,Z. and Lapusta,Y., On designing dielectric elastomer actuators. *Journal of Applied Physics*, 2008, 104(9): 093503.

[11] O'Halloran,A., O'Malley,F. and McHugh,P., A review on dielectric elastomer actuators, technology, applications, and challenges. *Journal of Applied Physics*, 2008, 104(7): 071101.

[12] Koh,S.J.A., Zhao,X. and Suo,Z., Maximal energy that can be converted by a dielectric elastomer generator. *Applied Physics Letters*, 2009, 94(26): 262902.

[13] Brochu,P. and Pei,Q., Advances in dielectric elastomers for actuators and artificial muscles. *Macromolecular Rapid Communications*, 2010, 31(1): 10-36.

[14] Koh,S.J.A., Li,T., Zhou,J., Zhao,X., Hong,W., Zhu,J. and Suo,Z., Mechanisms of large actuation strain in dielectric elastomers. *Journal of Polymer Science Part B: Polymer Physics*, 2011, 49(7): 504-515.

[15] Qiang,J.H., Chen,H.L. and Li,B., Experimental study on the dielectric properties of polyacrylate dielectric elastomer. *Smart Materials and Structures*, 2012, 21(2): 025006.

[16] Goulbourne,N., Mockensturm,E. and Frecker,M., A nonlinear model for dielectric elastomer membranes. *Journal of Applied Mechanics*, 2005, 72(6): 899-906.
[17] Dorfmann,A. and Ogden,R.W., Nonlinear electroelasticity. *Acta Mechanica*, 2005, 174(3): 167-183.
[18] Suo,Z., Zhao,X. and Greene,W.H., A nonlinear field theory of deformable dielectrics. *Journal of the Mechanics and Physics of Solids*, 2008, 56(2): 467-486.
[19] Trimarco,C., On the Lagrangian electrostatics of elastic solids. *Acta Mechanica*, 2009, 204(3): 193-201.
[20] Suo,Z., Theory of dielectric elastomers. *Acta Mechanica Solida Sinica*, 2010, 23(6): 549-578.
[21] Plante,J.S. and Dubowsky,S., Large-scale failure modes of dielectric elastomer actuators. *International Journal of Solids and Structures*, 2006, 43(25-26): 7727-7751.
[22] Foo,C.C., Cai,S., Koh,S.J.A., Bauer,S. and Suo,Z., Model of dissipative dielectric elastomers. *Journal of Applied Physics*, 2012, 111(3): 034102.
[23] Huang,J., Li,T., Foo,C.C., Zhu,J., Clarke,D.R. and Suo,Z., Giant, voltage-actuated deformation of a dielectric elastomer under dead load. *Applied Physics Letters*, 2012, 100(4): 041911.
[24] Zhao,X.H., Koh,S.J.A. and Suo,Z.G., Nonequilibrium thermodynamics of dielectric elastomers. *International Journal of Applied Mechanics*, 2011, 3(2): 203-217.
[25] Where do the 'Pure' and 'Shear' Come From in the Pure Shear Test? In: Fatigue Life Simulation for Rubber. www.endurica.com